AJNR Am J Neuroradiol 26:1532–1538, June/July 2005

Retrograde Cortical and Deep Venous Drainage in Patients with Intracranial Dural Arteriovenous Fistulas: Comparison of MR Imaging and Angiographic Findings

Mika Kitajima, Toshinori Hirai, Yukunori Korogi, Masayuki Yamura, Koichi Kawanaka, Ichiro Ikushima, Yoshiko Hayashida, Yasuyuki Yamashita, and Junichi Kuratsu

BACKGROUND AND PURPOSE: **We assessed MR imaging, specifically contrast-enhanced three-dimensional (3D) magnetization-prepared rapid gradient-echo (MP-RAGE), in evaluating retrograde venous drainage in patients with intracranial dural arteriovenous fistulas (dAVFs) that may result in catastrophic venous infarction or hemorrhage.**

METHODS: **Twenty-one patients with angiographically proved dAVFs underwent nonenhanced spin-echo (SE) and fast SE imaging, 3D fast imaging with steady-state precession, and enhanced SE and 3D MP-RAGE imaging. Retrograde venous drainage was categorized as cerebral cortical, deep cerebral, posterior fossa medullary, ophthalmic, or spinal venous. We assessed retrograde venous drainage and graded its severity. MR imaging and angiographic severities were correlated. Sensitivity, specificity, and accuracy were calculated to evaluate the diagnostic utility of each technique compared with conventional angiography. We retrospectively correlated angiograms and MR images.**

RESULTS: **Enhanced 3D MP-RAGE and T1-weighted SE images had higher diagnostic accuracy higher than nonenhanced images, especially when retrograde drainage involved cerebral cortical, posterior fossa, and spinal veins. Correlation of severity for enhanced MP-RAGE images and enhanced T1-weighted images with angiograms was good to excellent and better than that with nonenhanced images. All sequences had low diagnostic accuracy when drainage was via deep cerebral veins. On retrospective review, 3D MP-RAGE images showed two thrombotic inferior petrosal sinuses.**

CONCLUSION: **Enhanced MR images were superior to nonenhanced images in assessing retrograde venous drainage in intracranial dAVFs. Enhanced 3D MP-RAGE is superior to enhanced T1-weighted SE imaging for determining the route and severity of venous reflux because of its increased spatial resolution and ability to contiguously delineate the venous system.**

Dural arteriovenous fistulas (dAVFs), or dural shunts, were also called dural arteriovenous malformations before it was understood that almost all were acquired lesions (1). These lesions may cause various signs and symptoms ranging from pulsatile tinnitus to intracranial hemorrhage (1–10). dAVFs are due to impaired venous outflow that results in retrograde venous drainage and venous hypertension and, eventually, venous infarction with hemorrhage. Nonaggressive neurologic symptoms, such as isolated headache, vertigo, and bruit, are observed in more than 50% of patients with dAVFs, whereas aggressive neurologic symptoms intracranial hypertension, intracranial hemorrhage, focal neurologic deficits, and seizures are less common. The incidence of intracranial hemorrhage, the most critical symptom, is 7%–27% in patients with dAVF (1–3).

In patients with intracranial dAVFs and retrograde venous drainage, two major classifications based on the presence of retrograde leptomeningeal venous drainages have been proposed (2, 4). An increase in the direct retrograde venous drainage into a cortical

Received August 1, 2004; accepted after revision December 13.

From the Departments of Radiology (M.K., T.H., M.Y., K.K., I.I., Y.H., Y.Y.), and Neurosurgery (J.K.), Kumamoto University School of Medicine, Kumamoto, Japan; and the Department of Radiology, University of Occupational and Environmental Health, School of Medicine (Y.K.) Kitakyushu, Japan.

Address reprint requests to Mika Kitajima, MD, Department of Radiology, Kumamoto University School of Medicine, 1-1-1 Honjo, Kumamoto, Japan, 860-8556.

TABLE 1: Angiographic findings

Patient/Age (years)/Sex	Fistula Site	Feeding Artery	Obstructed Petrosal Sinus	Retrograde Drainage Veins
1/69/F	R/L CS	R/L ECA, ICA	R/L superior, inferior	Cortical, deep
2/66/F	R/L CS	R/L ECA, ICA	R/L superior, inferior	Cortical, deep
3/58/F	R/L CS	R/L ECA, ICA	R/L superior, inferior	Cortical, deep, superior ophthalmic, PF
4/62/F	L CS	R/L ECA, ICA	L superior, R/L inferior	Deep, superior ophthalmic, PF, SV
5/77/M	L CS	R/L ICA	R/L superior, inferior	Cortical, deep
6/51/F	R CS	R/L ECA, ICA	R/L superior, inferior	Superior ophthalmic
7/62/F	R CS	R/L ECA, ICA	R/L superior, inferior	Deep, superior ophthalmic
8/62/F	L CS	R/L ECA, ICA	R/L superior, inferior	Superior ophthalmic
9/76/F	R/L CS	R ICA, R/L ECA	R/L superior, inferior	Cortical, deep, superior ophthalmic, PF
10.52/M	R CS	R/L ECA	Not applicable	Cortical
11/50/F	L CS	L ECA	Not applicable	Superior ophthalmic
12/52/F	L CS	L ECA	R/L superior, inferior	Deep
13/70/F	L CS	L ECA, ICA	R/L superior, inferior	Superior ophthalmic
14/77/F	L CS	L ECA, ICA	L superior, R/L inferior	Cortical, deep
15/70/M	Tent	L ECA, ICA; R/L VA	[a]	Cortical, deep
16/64/M	L CS	L ECA, ICA	R/L superior, inferior	PF
17/50/F	L transverse sinus	L ECA, ICA; L	[a]	Cortical, deep, PF, SV, superior ophthalmic
18/70/F	L CS	R ECA, ICA	Not applicable	Superior ophthalmic, PF
19/78/F	L CS	R/L ECA, R, ICA	L inferior	Cortical, superior ophthalmic, SV
20/70/M	L sigmoid sinus	L ECA	[a]	Cortical, PF
21/71/F	R CS	R ECA, ICA	L inferior	Superior ophthalmic

Note.—PF, leptomeningeal vein of the posterior fossa; SV, spinal vein; VA, verbetral arteries.

[a] Obstruction was in the L sigmoid sinus and superior sagittal sinus (patient 15), R transverse sinus (patient 17), or R transverse sinus (patient 20).

vein was significantly related to a high incidence of hemorrhage (2, 8, 11, 12).

Although the diagnosis and assessment of dAVFs are based primarily on the results of conventional angiography, MR imaging is useful (13, 14). On T2-weighted spin-echo (SE) images, retrograde venous drainage is identified as prominent flow voids in the subarachnoid space. The involved sinuses are demonstrated as high-signal intensity on three-dimensional (3D) fast imaging with steady-state precession (FISP) (14). Two-dimensional time-of-flight venography and contrast-enhanced 3D magnetization-prepared rapid gradient-echo (MP-RAGE) sequences aid in the evaluation of veins and dural sinuses (15). Although different MR images can be used to assess normal and abnormal dural sinuses and veins shown in these reports, the sequence that is most appropriate for assessing retrograde venous drainage in patients with intracranial dAVFs remains unknown.

The purpose of this study was to evaluate the diagnostic accuracy of nonenhanced and contrast-enhanced SE, 3D FISP, and contrast-enhanced 3D MP-RAGE images in depicting retrograde venous drainage in patients with intracranial dAVFs.

Methods

Patients

Twenty-one consecutive patients (five men, 16 women; age range, 50–78 years; mean age, 64.6 years) with 21 angiographically proved dAVFs underwent MR imaging, including nonenhanced and enhanced SE or fast SE, 3D FISP, and enhanced 3D MP-RAGE sequences. Conventional angiography and MR examinations were performed within 0–65 days (mean, 13.6 days) of each other. All patients were examined for suspected dAVFs. Their clinical symptoms were exophthalmos and chemosis (n = 17), tinnitus (n = 2), dementia (n = 1), and worsening of visual acuity (n = 1).

Conventional Angiography

Conventional angiography was performed by using digital subtraction angiography (DSA) with bilateral selective catheterization of the external carotid arteries (ECAs) and internal carotid arteries (ICAs) and vertebral arteries (VAs). Fistula sites were the tent (n = 1) and the unilateral cavernous (n = 14), bilateral cavernous (n = 4), transverse (n = 1), and sigmoid (n = 1) sinuses. All 21 patients had retrograde venous drainage. The routes were the deep venous system (n = 11) and the superior ophthalmic (n = 12), cerebral cortical (n = 11), posterior fossa (n = 7), and spinal (n = 3) veins (Table 1).

Two radiologists (Y.K., M.K.) graded the severity of the retrograde cortical venous drainage in consensus, as follows: grade 0 = no retrograde cortical venous drainage, grade 1 = involved volume of 0–25%, grade 2 = 26–50%, and grade 3 = >50%. The volume of involved cortical veins was visually determined visually relative to the whole of the cortical veins on the anteroposterior and lateral angiograms. Ten patients had no retrograde cortical venous drainage, two patients had grade 1 drainage, seven patients grade 2, and two patients had grade 3.

In 15 patients with carotid cavernous fistulas, the superior and/or inferior petrosal sinuses were not seen during the venous phase. The superior sagittal sinus was not seen in one patient with a tentorial dAVF, and the sigmoid and transverse sinuses were not visualized in two patients with transverse and/or sigmoid sinus dAVFs.

MR Imaging

MR examinations were performed with a 1.5-T superconducting unit (Magnetom Vision; Siemens, Erlangen, Germany). In all patients, axial T1-weighted (TR/TE/NEX = 627–690/14–17/1) SE and T2-weighted (3700/96/1, echo train length = 7) fast SE images of the entire brain were obtained. SE images were obtained with a 21-cm field of view (FOV) and a 224 × 256 matrix. Section thickness was 5 mm with a 1-mm

intersection gap. In 19 patients, contrast-enhanced T1-weighted SE images were also obtained after the administration of gadopentetate dimeglumine (0.1 mmol/kg; Magnevist; Nihon Schering, Osaka, Japan) with a same parameters as those used for nonenhanced T1-weighted imaging.

All patients underwent 3D FISP imaging. The parameters were TR/TE = 32/6.5, 20° flip angle, 64-mm slab thickness, 64 partitions, 20-cm FOV, and 192–256 × 256–512 matrix. Zero-fill interpolation was applied in the section selection direction, and the section thickness was 0.5 mm. The cavernous sinus (CS) was located at the center of the volume slab.

Contrast-enhanced 3D MP-RAGE images were also obtained in all patients, with TR/TE/TI = 13.5/7/3000, 15° flip angle, 135-mm slab thickness, 108 partitions, 20-cm FOV, and 224 × 256 matrix. The section thickness was 1.3 mm. The center of the slab was same as that of the 3D FISP images.

Image Interpretation

Two readers (M.Y., K.K.) who were cognizant of the presence of dural fistulas but not their sites reviewed the SE, 3D FISP, and enhanced 3D MP-RAGE images in random order. During their assessment of individual images, they did not have access to information obtained with other techniques or conventional angiography or from the clinical records. They recorded the presence of retrograde venous drainage, as shown on all images. When this drainage was identified, its route was noted by using conventional angiographic classification, and its severity was assessed.

Diagnostic criteria for retrograde venous drainage were abnormal flow voids on T2-weighted fast SE images, hyperintensity of veins on 3D FISP images, and laterality of the vein size on nonenhanced and enhanced T1-weighted SE and enhanced 3D MP-RAGE images. To differentiate veins from arteries, the readers paid careful attention to the anatomic location and tortuosity of the vessels.

In the retrospective qualitative study, two radiologists (Y.K., M.K.) who were cognizant of the patient's history interpreted the MR image and angiogram together. They assessed the patency of the dural sinuses, particularly in the superior and inferior petrosal sinuses, and noted abnormal parenchymal intensity associated with venous congestion.

Data Analysis

First, to determine interobserver variability, the degree of agreement between the observers was analyzed by using κ statistics. κ values of up to 0.4 were recorded as positive, but poor correlation, 0.41–0.75 was good and >0.75 was excellent. Second, the sensitivity, specificity, and accuracy of each imaging technique were calculated to assess its diagnostic utility compared with that of conventional angiography as the standard. In patients with retrograde cortical venous drainage, we used κ statistics to compare its severity on conventional angiograms and on the various MR images.

Results

Confidence levels for image interpretation by the two readers were 0.9–1.0 for T1-weighted images, 0.76–0.95 for T2-weighted images, 0.73–1.0 for enhanced T1-weighted images, 0.81–1.0 for 3D FISP images, and 0.65–1.0 for enhanced 3D MP-RAGE images. All κ values, except for those from the evaluation of ophthalmic veins on enhanced T1-weighted image and of deep veins on enhanced MP-RAGE images, were more than 0.75. Table 2 shows the sensitivity, specificity, and accuracy of each imaging technique.

TABLE 2: Mean sensitivity, specificity, and accuracy judged by two observers

Vein[a]	Sensitivity (%)	Specificity (%)	Accuracy (%)
Cortical			
T1 weighted	50	100	73.8
T2 weighted	77.3	100	88.1
CE T1 weighted	100	100	100
3D FISP	77.3	86.7	85.7
3D CE MP-RAGE	100	90	95.3
Ophthalmic			
T1 weighted	91.7	100	95.2
T2 weighted	66.7	94.5	78.6
CE T1 weighted	40.0	100	68.5
3D FISP	45.9	100	69.1
3D CE MP-RAGE	91.7	83.4	88.1
Deep			
T1 weighted	13.4	100	54.8
T2 weighted	47.3	100	69.1
CE T1 weighted	34.7	95.0	68.4
3D FISP	46.8	95.5	69.1
3D CE MP-RAGE	51.4	85.0	69.1
Posterior			
T1 weighted	25.9	100	73.8
T2 weighted	25.9	100	73.8
CE T1 weighted	50.0	96.5	81.6
3D FISP	18.8	96.5	69.1
3D CE MP-RAGE	59.0	82.3	76.2
Spinal			
T1 weighted	0	100	85.7
T2 weighted	16.7	100	85.7
CE T1 weighted	75.0	100	94.8
3D FISP	0	100	85.7
3D CE MP-RAGE	100	100	100

[a] CE = contrast enhanced.

For the evaluation of cerebral retrograde cortical venous drainage, enhanced T1-weighted SE and enhanced 3D MP-RAGE images yielded diagnostic accuracy higher than that of the other techniques (Fig 1). For the evaluation of the ophthalmic vein, nonenhanced T1-weighted SE and 3D MP RAGE images were superior (Fig 2). All sequences had relatively low diagnostic accuracy for the evaluation of deep veins (Fig 3). Enhanced 3D MP-RAGE images were more sensitive than the other images for evaluating posterior fossa and spinal veins (Figs 3 and 4), although their specificity for the veins in the posterior fossa was relatively low. Diagnostic accuracy for all reflux routes was 85.7% on enhanced MP-RAGE, 82.7% on enhanced T1-weighted SE, 79.1% on T2-weighted fast SE, 76.7% on nonenhanced T1-weighted SE, and 75.7% on 3D FISP imaging. In evaluating the severity of cortical retrograde venous drainage, good-to-excellent correlation was observed among enhanced MP-RAGE images, enhanced T1-weighted images, and angiograms for both readers. κ values were >0.594 with both MR sequences. κ values for the other sequences were 0.132–0.465.

In our retrospective evaluation, enhanced MP-RAGE images were particularly useful for assessing the small veins of the posterior fossa and for identifying thrombosis in the dural sinuses. In four patients,

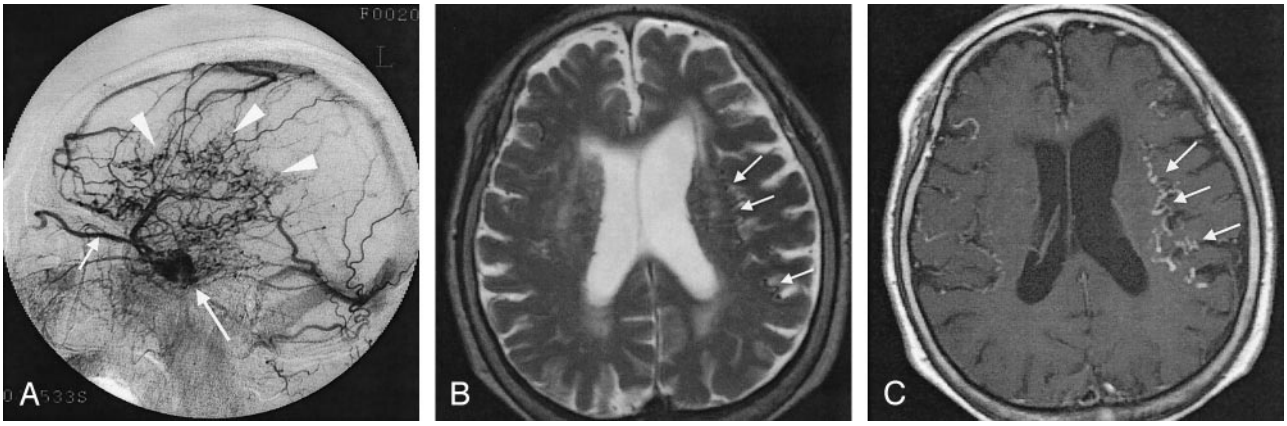

FIG 1. Case 19. A 78-year-old woman with dAVF in the left CS.

A, Lateral intra-arterial DSA of the left ECA shows the arteriovenous shunt in the left CS (*long arrow*) and retrograde venous drainage to the superior ophthalmic vein (*short arrow*) and cerebral cortical veins (*arrowheads*). Severity of the drainage was grade 2 (26%–50% of cortical veins on angiography).

B, Axial T2-weighted SE MR image shows flow voids (*arrows*) in the subarachnoid space, suggesting dilated cortical veins in bilateral frontal and parietal lobes.

C, Abnormal dilated cortical veins (*arrows*) are more prominent on this axial enhanced T1-weighted SE image than in *B*.

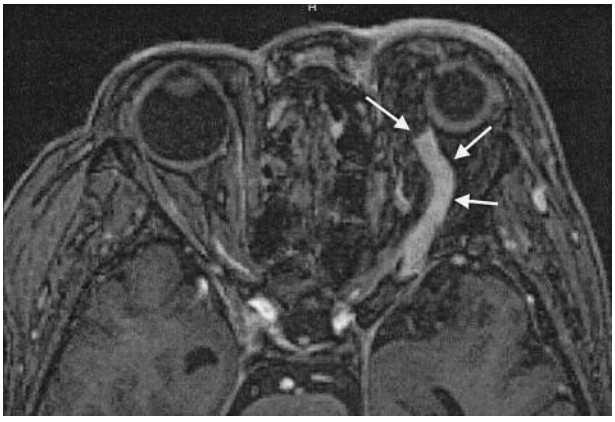

FIG 2. Case 13. A 70-year-old woman with dAVF in the left CS. Enhanced 3D MP-RAGE image clearly shows marked dilatation and thrombus in the anterior part of the left superior ophthalmic vein (*arrows*).

enhanced 3D MP-RAGE images showed filling defects in the inferior petrosal sinuses. In patients 1 and 3, the sinuses were hypointense on 3D FISP images but not opacified conventional angiographs, even in the late venous phase; this appearance was considered to reflect sinus thrombosis (Fig 5). In patients 6 and 21, the inferior petrosal sinuses were hyperintense on 3D FISP images; high flow in the sinuses was confirmed on conventional angiographs. With respect to parenchymal changes, the temporal white matter adjacent to the area of retrograde venous drainage was hyperintense on T2-weighted fast SE images in patients 19 and 20.

Discussion

Impairment of venous outflow in patients with dAVFs results in retrograde venous drainage and venous hypertension and eventual venous infarction with hemorrhage. Two major classifications have been proposed on the basis of retrograde leptomeningeal venous drainage. Cognard et al (2) reviewed findings in 205 patients and found a relationship between the type of retrograde venous drainage and the clinical presentation. Patients with dAVFs draining directly into a cortical vein had a high incidence of hemorrhage, particularly those with venous ectasia. Other groups that examined the correlation between the severity of retrograde venous drainage and clinical presentations showed that direct retrograde leptomeningeal venous drainage results in an incidence of hemorrhage higher than that of sinosal drainage with retrograde leptomeningeal venous drainage (4, 6–12).

Evaluation of retrograde venous drainage on conventional angiography requires good visualization in the venous phase. Retrograde venous drainage is identified as abnormally dilated, tortuous, engorged pial or medullary veins in the late venous phase; this is known as the pseudophlebitic pattern. Other conventional angiographic findings in patients with dAVFs are focal regions of delayed circulation and venous rerouting to the orbit or to transosseous veins. Abnormally dilated pial or medullary veins in patients with dAVFs are identified as flow void on T2-weighted SE images. Willinsky et al (13) attempted to correlate the severity of retrograde venous drainage determined on T2-weighted SE images with the clinical presentation and suggested that evidence of moderate or severe retrograde venous drainage may be useful for identifying a subgroup of patients in whom aggressive symptoms or signs might develop.

Our study showed that enhanced MR images were superior to nonenhanced images for evaluating retrograde venous drainage, probably because undilated veins and slow flow retrograde venous drainage may not be detected with T2-weighted SE images. Both enhanced 3D MP-RAGE and T1-weighted SE images had high diagnostic accuracy, not only for the detection of retrograde cortical venous drainage but also for its severity. Although

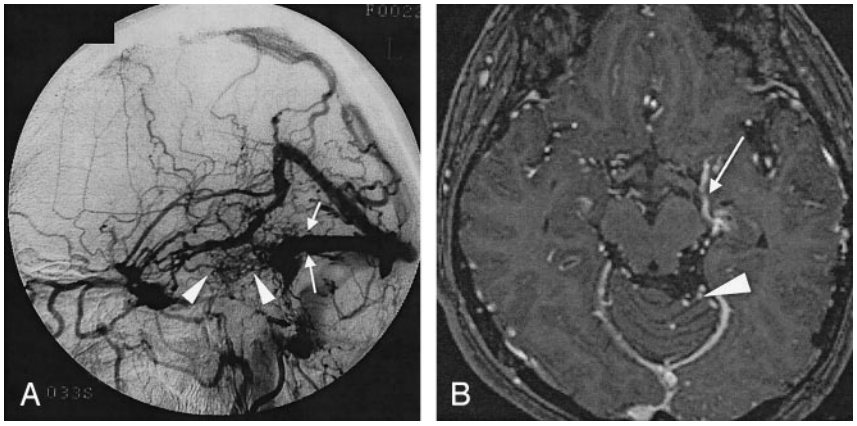

FIG 3. Case 17. A 50-year-old woman with dAVF in the left transverse sinus.

A, Lateral intra-arterial DSA of the left ECA shows obstruction of the left transverse sinus (*arrows*). Abnormal vessels (*arrowheads*) are observed around the obstructed left transverse sinus. Severity of the drainage was grade 2 (26%–50% of cortical veins on angiography).

B, Enhanced 3D MP-RAGE image shows abnormal dilated veins at the base of the cerebrum (*arrow*) and in the posterior fossa (*arrowhead*). Bilateral posterior cerebral arteries were identified on other sections (not shown).

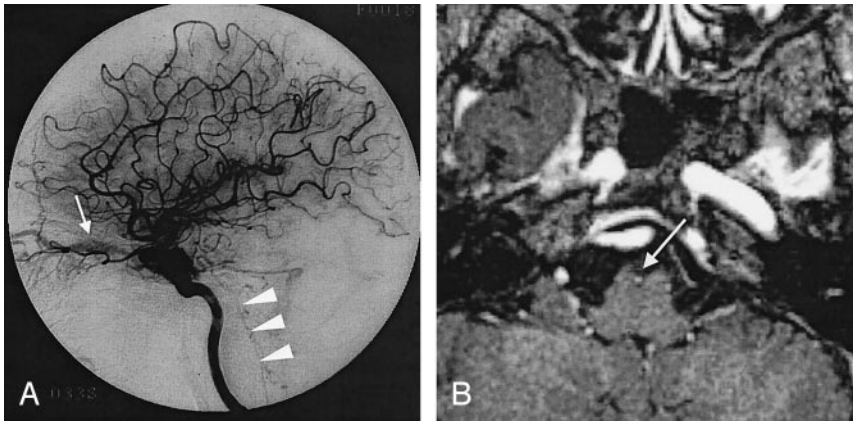

FIG 4. Case 4. A 62-year-old woman with dAVF in the left CS.

A, Lateral intra-arterial DSA of the left ICA shows retrograde venous drainage to the superior ophthalmic (*arrow*) and pontomedullary (*arrowheads*) veins.

B, Enhanced 3D MP RAGE image shows cephalocaudal, contiguous enhancing structures (*arrow*) at the ventral side of midbrain corresponding to retrograde venous drainage to the pontomedullary vein.

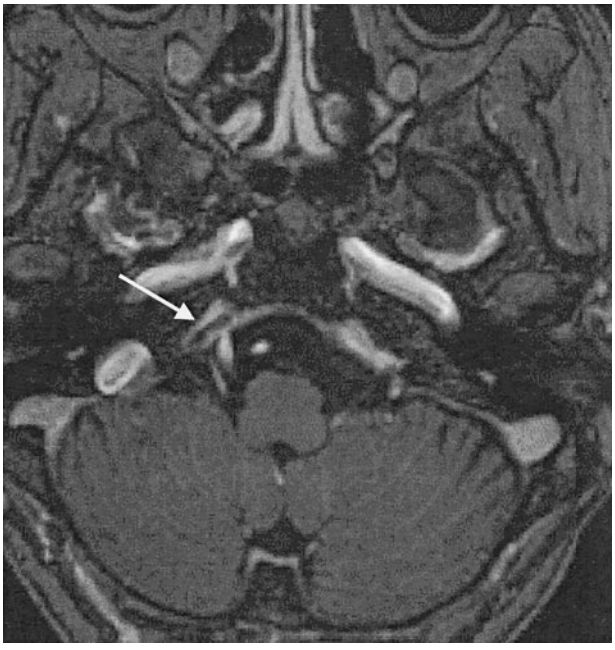

FIG 5. Case 3. A 58-year-old woman with dAVF in the bilateral CSs. Enhanced 3D MP-RAGE image (and 3D FISP image, not shown) depicts a filling defect in the right inferior petrosal sinus (*arrow*). This finding suggests thrombosis in the right inferior petrosal sinus.

enhanced 3D MP-RAGE images were highly sensitive, their specificity was slightly lower than that of enhanced T1-weighted SE images.

3D MP-RAGE is a small–flip angle, gradient-recalled-echo sequence in which a 3D Fourier transformation acquisition is implemented with a 180° inversion preparation pulse. The resulting sequence yields heavily T1-weighted contrast; a relatively high signal-to-noise ratio; thin, continuous images with postprocessing capability; rapid acquisition times; and depiction of flow-related enhancement (16–20). Enhanced 3D MP-RAGE sequence relies not only on time-of-flight effects but also on the T1-reducing effect of gadolinium to depict the flow (21). Although these effects are beneficial for identifying normal vasculature on enhanced 3D MP RAGE images, it may make the differentiation of normal and affected veins more difficult than it is on enhanced T1-weighted SE images. Therefore, enhanced 3D MP-RAGE imaging is slightly less specific than enhanced T1-weighted SE imaging.

3D FISP and T2-weighted SE images had relatively high diagnostic accuracy in patients with cerebral retrograde cortical venous drainage. On 3D FISP images, high-flow vessels had high signal intensity attributable to flow-related enhancement, which is advantageous for evaluating high-flow retrograde venous drainage (14, 22). Although 3D FISP images have a high spatial resolution (0.5 mm) and detectability of high flow is high, they have drawbacks: their acquisition time is long; the slab thickness is limited; and, on peripheral images in the slab, the signal intensity of even high-flow vessels is decreased because

of saturation effect. These limitations may account for the lower diagnostic accuracy of 3D FISP images than on enhanced images.

In the evaluation of the ophthalmic vein, enhanced 3D MP-RAGE images had relatively high diagnostic accuracy. On enhanced 3D MP-RAGE images, the fat-suppression effect improves delineation of intraorbital structures. Enhanced images were more accurate than nonenhanced images for the diagnosis of retrograde venous drainage to the posterior fossa. Enhanced 3D MP-RAGE images were more sensitive than T1-weighted SE images because of the high spatial resolution with no gaps, the reduction of vascular dephasing, the decreased susceptibility artifacts, and the suppression of fat signals (19). Although our study population included only three patients with retrograde venous drainage to the pontomedullary vein, detection of this was possible only on enhanced 3D MP-RAGE images, possibly because their high spatial resolution and decreased phase artifact.

The diagnosis of retrograde venous drainage into deep veins was difficult regardless of the imaging technique used. Although all images were highly specific, detection was possible in only half of our patients, even on enhanced 3D MP-RAGE images. This result suggested a visualization overlap on MR images between normal veins and veins with retrograde drainage. Many veins and sinuses, such as the sphenoparietal sinus entering into the deep venous systems, and their direction and volume of flow are complex, even in healthy individuals.

On retrospective study, abnormal findings in the inferior petrosal sinuses were observed in four patients. Assessment of the petrosal sinus is important in patients with intracranial dAVFs. In those with carotid-cavernous dural fistula, thrombosis or occlusion of the posterior drainage leads to increased anterior drainage, which results in worsening of exophthalmus and/or chemosis. Furthermore, in patients with dAVFs, interventional curative procedures involve embolization of the affected sinuses and draining routes (23, 24), and the inferior petrosal sinus is one of the most frequent routes used for the transvenous approach. Therefore, enhanced 3D MP-RAGE images may be useful for evaluating veins and sinuses before interventional procedures.

Our study had some limitations. First, most of the lesions were dAVFs at the CS; therefore, our results might not be applicable to fistulas in other sites. In our three patients with fistulas in other sites, however, retrograde venous drainage was well delineated on enhanced MP-RAGE images. Because retrograde venous drainage of dAVFs are similarly seen regardless of the location of the fistula location, we believe that our results are applicable to dAVFs at any location. Evaluation of dAVFs at locations other than the carotid cavernous region is also desirable. Second, we included only patients with known retrograde venous drainage, as confirmed on conventional angiography. Therefore, the incidence of false-positive findings was not fully established. A large sample of dAVFs with or without retrograde venous drainages should be evaluated to establish the actual rates of sensitivity and specificity. Third, enhanced MP-RAGE images cannot provide hemodynamic information equivalent to that obtained with intra-arterial conventional angiography. Although advances have made demonstration of cerebral hemodynamics on MR imaging equivalent to that of intra-arterial conventional angiography (25, 26), we suggest that enhanced high-resolution images, particularly 3D MP-RAGE images, are best for evaluating the retrograde venous drainage in patients with intracranial dAVFs.

Conclusion

Contrast-enhanced MR images are superior to nonenhanced images for assessing retrograde venous drainage in patients with intracranial dAVFs. Enhanced 3D MP-RAGE imaging, which provides high spatial resolution and contiguous depiction of the venous system, may be better than enhanced T1-weighted SE imaging for understanding the routes and severity of retrograde venous drainage. In addition, to evaluate sinus patency, the enhanced 3D MP-RAGE sequence was more appropriate than others.

References

1. Vinuela F, Fox AJ, Pelz DM, Drake CG. **Unusual clinical manifestations of dural arteriovenous malformations.** *J Neurosurg* 1986;64:554–558
2. Cognard C, Gobin YP, Pierot L, et al. **Cerebral dural arteriovenous fistulas: clinical and angiographic correlation with a revised classification of venous drainage.** *Radiology* 1995;194:671–680
3. Obrador S, Soto M, Silvela J. **Clinical syndromes of arteriovenous malformations of the transvers-sigmoid sinus.** *J Neurol Neurosurg Psychiatry* 1975;38:436–451
4. Borden JA, Wu KW, Shucart WA. **A proposed classification for spinal and cranial dural arteriovenous fistulous malformations and implications for treatment.** *J Neurosurg* 1995;82:166–179
5. Lasjaunias P, Chiu M, terBrugge K, et al. **Neurological manifestations of intracranial dural arteriovenous malformations.** *J Neurosurg* 1986;64:724–730
6. Cognard C, Casasco A, Toevi M, et al. **Dural arteriovenous fistulas as a cause of intracranial hypertension due to impairment of cranial venous outflow.** *J Neurol Neurosurg Psychiatry* 1998;65:308–316
7. Davies M, terBrugge K, Willinsky RA, et al. **The validity of classifications for the clinical presentations of intracranial dural arteriovenous fistulas.** *J Neurosurg* 1996;85:830–837
8. Brown R, Wiebers DO, Nichols D. **Intracranial dural arteriovenous fistulae: angiographic predictors of intracranial hemorrhage and clinical outcome in nonsurgical patients.** *J Neurosurg* 1994;81:531–538
9. Hurst RW, Bagley LJ, Galetta S, et al. **Dementia from dural arteriovenous fistulas: the pathologic findings of venous hypertensive encephalopathy.** *AJNR Am J Neuroradiol* 1998;19:1267–1273
10. Ishii K, Goto K, Ihara K, et al. **High-risk dural arteriovenous fistulae of the transverse and sigmoid sinuses.** *AJNR Am J Neuroradiol* 1987;8:1113–1120
11. Awad IA, Little JR, Akrawi WP, Ahl J. **Intracranial dural arteriovenous malformations: factors predisposing to an aggressive neurological course.** *J Neurosurg* 1990;72:839–850
12. Barnwell SL, Halbach VV, Dowd CF, et al. **A variant of arteriovenous fistulas within the wall of dural sinuses: results of combined surgical and endovascular therapy.** *J Neurosurg* 1991;74:199–204
13. Willinsky R, Goyal M, terBrugge K, Montanera W. **Tortuous, engorged pial veins in intracranial dural arteriovenous fistulas: correlations with presentation, location, and MR findings in 122 patients.** *AJNR Am J Neuroradiol* 1999;20:1031–1036
14. Hirai T, Korogi Y, Hamatake S, et al. **Three-dimensional FISP**

imaging in the evaluation of carotid cavernous fistula: comparison with contrast-enhanced CT and spin-echo MR. *AJNR Am J Neuroradiol* 1998;19:253–259
15. Liang L, Korogi Y, Takahashi M, et al. **Evaluation of the intracranial dural sinuses with a 3D contrast-enhanced MP-RAGE sequence: prospective comparison with 2D-TOF venography and digital subtraction angiography.** *AJNR Am J Neuroradiol* 2001;22:481–492
16. Brant-Zawadzki M, Gillan GD, Nitz WR. **MP RAGE: a three-dimensional, T1-weighted, gradient-echo sequence: initial experience in the brain.** *Radiology* 1992;182:769–775
17. Fellner F, Holl K, Held P, et al. **A T1-weighted rapid three-dimensional gradient-echo technique (MP-RAGE) in preoperative MRI of intracranial tumors.** *Neuroradiology* 1996;38:199–206
18. Brant-Zawadzki M, Gillan GD, Atkinson DJ, et al. **Three-dimensional MR imaging and display of intracranial disease: improvements with the MP-RAGE sequence and gadolinium.** *J Magn Reson Imaging* 1993;3:656–662
19. Runge VM, Kirsch JE, Thomas GS, Mugler JP. **Clinical comparison of three-dimensional MP-RAGE and FLASH techniques for MR imaging of the head.** *J Magn Reson Imaging* 1991;1:493–500
20. Mirowitz SA. **Intracranial lesion enhancement with gadolinium: T1-weighted spin-echo versus three-dimensional Fourier transform gradient-echo MR imaging.** *Radiology* 1992;185:529–534
21. Stevenson J, Knopp EA, Litt AW. **MP-RAGE subtraction venography: a new technique.** *J Magn Reson Imaging* 1995;5:239–241
22. Chen J, Tsuruda JS, Halbach VV. **Suspected dural arteriovenous fistula: results with screening MR angiography in seven patients.** *Radiology* 1992;183:265–271
23. Vinuela F, Fox A, Debrun G, et al. **Spontaneous carotid-cavernous fistulas: clinical, radiological, and therapeutic considerations.** *J Neurosurg* 1984;60:976–984
24. Kiyosue H, Hori Y, Okahara M, et al. **Treatment of intracranial dural arteriovenous fistulas: current strategies based on location and hemodynamics, and alternative techniques of transcatheter embolization.** *Radiographics* 2004;24:1637–1653
25. Aoki S, Yoshikawa T, Hori M, et al. **Two-dimensional thick-slice MR digital subtraction angiography for assessment of cerebrovascular occlusive diseases.** *Eur Radiol* 2000;10:1858–1864
26. Yoshikawa T, Aoki S, Hori M, et al. **Time-resolved two-dimensional thick-slice magnetic resonance digital subtraction angiography in assessing brain tumors.** *Eur Radiol* 2000;10:736–744